Experimental and Theoretical Study of the Structural, Magnetic and Electronic Properties of the Ba_2GdSbO_6 Perovskite

R. Moreno Mendoza, D. A. Landínez Téllez, R. Cardona, L. A. Carrero Bermúdez and J. Roa-Rojas*

* *jroar@unal.edu.co*

Received: April 2016 Accepted: April 2017

Grupo de Física de Nuevos Materiales, Departamento de Física, Universidad Nacional de Colombia, Bogotá D.C., AA 5997, Colombia.

DOI: 10.22068/ijmse.14.2.1

Abstract: *In this work the procedure to the synthesis of Ba_2GdSbO_6 complex perovskite by the solid-state reaction method is reported. Theoretically a study of the crystalline and electronic structure was performed into the framework of the Density Functional Theory (DFT). The most stable structure is obtained to be a rhombohedral perovskite with a lattice constant a=6,0840 Å. Due the occurrence of a mean energy gap of 2,84 eV close to the Fermi level for both up and down spin polarizations this material is classifies as insulator. The effective magnetic moment of material obtained from the calculations was 7,0 μ_B. The crystalline structure was analyzed through the X-ray diffraction technique and Rietveld refinement of the experimental data. Results are strongly in agreement with those theoretically predicted. Magnetic response was studied from measurements of magnetic susceptibility as a function of temperature. Results reveal the paramagnetic feature of this material in the temperature regime from 50 K up to 300 K. From the fitting with the Curie law the effective magnetic moment was obtained to be 8,1 μ_B, which is slightly higher that the theoretical value for the Gd^{3+} isolated cation predicted by the theory of paramagnetism. The energy gap obtained from experiments of diffuse reflectance is relatively in agreement with the theoretical predictions. The dielectric constant as a function of applied frequencies at room temperature was measured. Results reveal a decreasing behavior with a high value of dielectric constant at low applied frequencies.*

Keywords: *Perovskite Material, Structure, Magnetic Feature, Electronic Properties*

1. INTRODUCTION

Recently, there has been a great interest in the electronic oxide ceramics oxides with ABO_3 perovskite structure due to the chemical versatility to evaluate different combinations of transition metal cation in the B site and obtain a variety of magnetic and electric properties [1, 2]. Ideally, a simple ABO_3 perovskite possesses a 3-dimensional cubic network of BO_6 octahedra with the cation A into the void formed by eight octahedral with AO_{12} coordination [3]. If the A and B sites contain a mixture of cations, distorted complex perovskites structures with lower symmetries are obtained. Distortions are mainly related with octahedral tilting due to a small cation driving a rotating of octahedral respect the crystallographic axes. Other kind of distortion is the cation displacement caused through first and second-order Jahn-Teller effects. Specially, the 1:1 B-site based class with chemical formula $A_2BB'O_6$ (or double perovskites) is the most frequently complex perovskite encountered [4]. From the distortions and composition of the double perovskites, new properties and applications are found in ferroelectric devices with large dielectric constants and frequency dispersion [5], magnetoresistance [6], solar energy conversion [7], catalysis [8], solid-oxide fuel cells [9] and microwave resonator [10]. In this paper we propose the synthesis and characterization of Ba_2GdSbO_6 ceramic material. We describe the crystalline structure of this double perovskite and perform morphological and compositional analyses. Furthermore, we present results of measurements of the magnetic response as a function of temperature. Moreover, considering that in recent years the density functional theory (DFT) has constituted in a strong tool to study electronic properties in

perovskite-like material [11], we carried out a study of the electronic properties of these materials, in order to establish the type of hybridization between the orbitals of GdO_6 and SbO_6 octahedra present in the structure.

2. EXPERIMENTAL

Samples were synthesized through the standard solid-state reaction recipe. Precursor powders of Gd_2O_3, Sb_2O_5 and Ba_2CO_3 (Aldrich 99.9%) were stoichiometrically mixed according to the chemical formula Ba_2GdSbO_6. Mixture was ground to form a pellet and annealed at 1000 ºC for 30 h. The samples were then regrinded, repelletized and sintered at 1100 ºC for 40 h and 1200 ºC for 40 h. X-ray diffraction (XRD) experiments were performed by means of a PW1710 diffractometer with λ_{CuK}=1,54064 Å. Rietveld refinement of the diffraction patterns was carried out by the GSAS program [12]. Morphological studies were performed by means scanning electron microscopy (SEM) experiments through the utilization of VEGA 3 equipment, and chemical composition of samples was analyzed by energy dispersive X-ray (EDX) technique. Field cooling measurements of the magnetic susceptibility as a function of temperature were carried out by using an MPMS Quantum Design SQUID. Diffuse reflectance experiments were performed by using a VARIAN Cary 5000 UV-Vis-NIR spectrophotometer, which has an integration sphere with a PMT/Pbs detector. The relative dielectric constant was measured by using an Agilent HP4194A-350 frequency analyzer.

3. CALCULATION METHOD

In order to determine the electronic and band structures we applied the Full-Potential Linear Augmented Plane Wave method (FP-LAPW) within the framework of the Kohn-Sham Density Functional Theory (DFT) [13], and adopted the Generalized Gradient (GGA) approximation for the exchange-correlation energy due to Perdew, Burke and Ernzerhof [14]. The self-consistent process is developed by the numeric package Wien2k [13]. Taking the experimental unit cell data as input, the structure studied in this work were fully relaxed with respect to their lattice parameters and the internal degrees of freedom compatible with the space group symmetry of the crystal structure. The resulting energies versus volume functions have been fitted to the equation of state due to Murnaghan [15] in order to obtain de minimum energy value, the bulk modulus, its pressure derivative and the equilibrium lattice parameters and associated volume. The muffin-tin radiuses used for Ba_2GdSbO_6 were 2,20; 2,50; 2,12 and 1,82 Bohr for Ba, Gd, Sb and O respectively, angular momentum up to l = 10 inside the muffin-tin sphere, a maximum vector in the reciprocal space of Gmáx=12,0; $RMT*K_{max}$ = 7,0 and a mesh of 1000 points in the first Brillouin zone (equivalent to a maximum of 250 k points in the irreducible Brillouin zone). Finally, the convergence criterion for the self-consistent calculation was 0,0001 Ry for the total energies, 0,0001 Bohr in the charge and 1,0 mRy/u.a in the internal forces. Spin polarization was included in the calculations.

4. RESULTS AND DISCUSSION

Figure 1 shows the XRD patterns obtained for Ba_2GdSbO_6. In the picture black symbols represent the experimental data and line corresponds to simulated pattern by means of GSAS code. Base line is the difference between theoretical and experimental results. Refinement parameters of figure 1 were x^2=5,236, $R_{(F2)}$=5,84%. From the Rietveld refinement it was established that these materials crystallize in a rhombohedral perovskite structure, space group R-3 (#148). The structural parameter obtained from the refinement was a=5,9882(1) Å. These results are 99,3% in agreement with the theoretical values obtained from the Structure Prediction Diagnostic Software SPuDS [16], which predicts a=6,0293 Å and α=57,8634º. In these ceramic materials the explanation of distortion from the ideal cubic perovskite structure is clear because the double perovskite have the generic formula $A_2BB'O_6$, and for this type of material the tolerance factor τ, is

[DOI: 10.22068/ijmse.14.2.1]

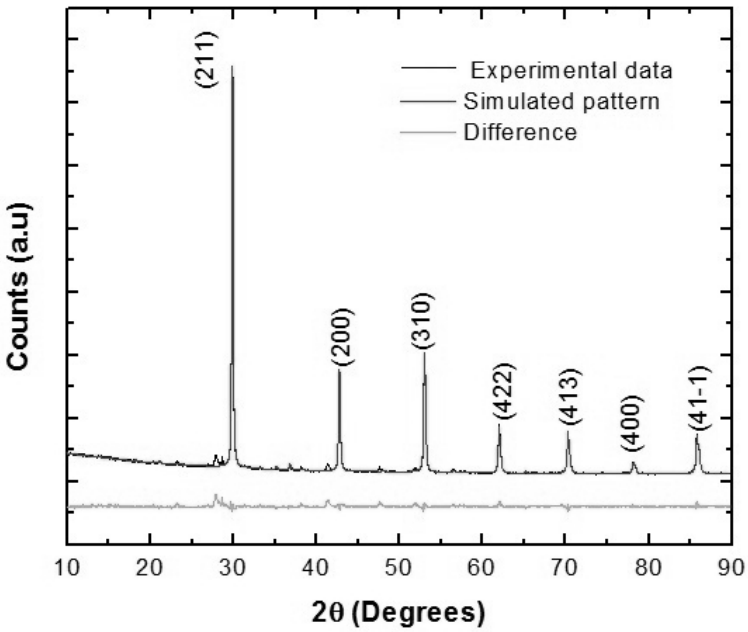

Fig. 1. Characteristic XRD pattern for the Ba2GdSbO6 double perovskite. Black symbols represent experimental diffraction data, continuous lines are the simulated patterns and base line is the difference between experimental and calculated values.

calculated by the ratio $\tau = \frac{r_A + r_o}{\sqrt{2}\left(\frac{r_B + r_{B'}}{2} + r_o\right)}$, where r_A, r_B, $r_{B'}$ and r_o are the ionic radii of the A, B, B', and O ions, respectively.

If τ is equal to unity, there is ideal cubic perovskite structure, and if τ<1 the structures is distorted from the cubic symmetry. The value of tolerance factor obtained for the complex perovskite was 0,9081. The Wyckoff positions obtained from the refinement analysis are presented in table 1.

From the structural analysis above, the expected structure of the Ba_2GdSbO_6 complex perovskite is that presented in figure 2. Clearly, a tolerance factor as far from the ideal value is related to distortions from the cubic cell. As showed in figures 2a and 2b, there is a difference between directions of the GdO_6 and SbO_6 octahedra. The most important has to do with the nature of the rhombohedral structure, since the trigonal angle α=60,0290º is quite far from 90o degrees corresponding to the ideal cubic cell. Furthermore, the tilt of the GdO_6 and SbO_6 octahedra occurs out of phase for an angle β=-16,4650º, corresponding to the Glazer notation a−a−a−, whose symmetry involves reflections, signaling odd-odd-odd reflections, which is characterized by cationic ordering and simple

Table 1. Atomic positions of cations and anions on the unit cell for Ba2GdSbO6.

Atom	Wyckoff Site	*x*	*y*	*z*
Ba	*2c*	0,2500	0,2500	0,2500
Gd	*1a*	0,0000	0,0000	0,0000
Sb	*1a*	0,5000	0,5000	0,5000
O1	*6f*	-0,1771	-0,3613	0,2705

[DOI: 10.22068/ijmse.14.2.1]

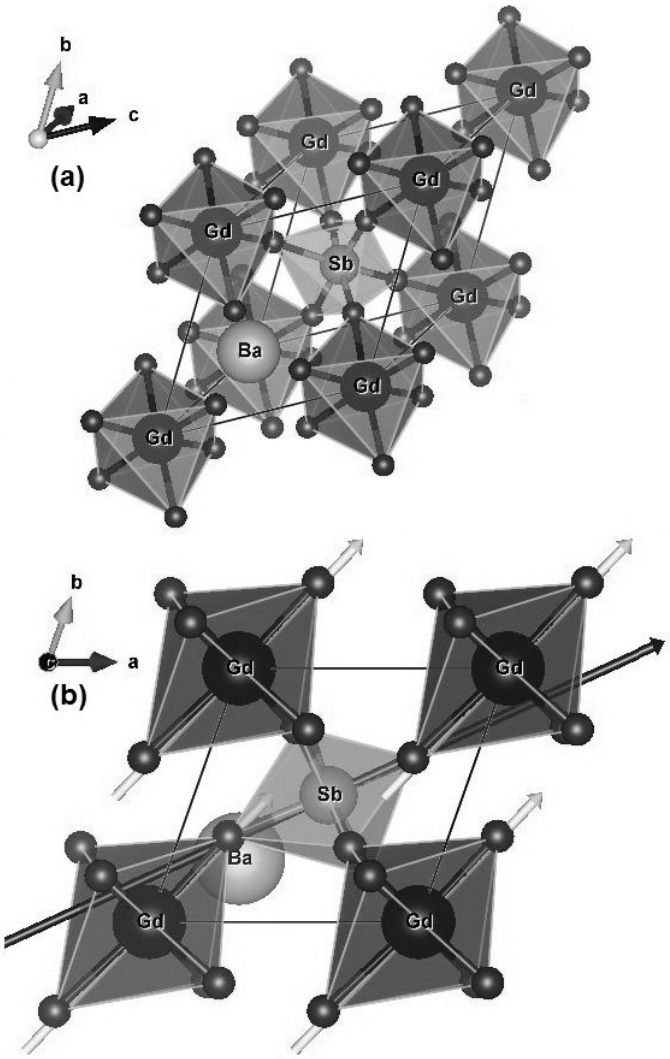

Fig. 2. (a) Characteristic cell and (b) GdO_6 and SbO_6 octahedra in the ab-plane for trigonal structure of the Ba2GdSbO6 double perovskite

octahedral tilting.

SEM images of the material shown in figure 3 reveal a qualitative approximation to the surface microstructure. In picture (a) evidences the formation of clusters of polyhedral grains and interstitial particulate grains. From picture (b) it is clear that the grains could end up having a few tens of nm, forming groups, which have appearance of clusters of several μm sizes.

By applying the EDX microprobe of the VEGA3 TESCAN microscope, the percentages of the constituent elements of the material were obtained, as reported in table 2. These values confirm that the material does not contain other elements than those corresponding to the expected stoichiometry Ba_2GdSbO_6. However, the experimental result reveals an apparent low content of the oxygen anion against an increase in the percentage of Ba, Gd and Sb cations, which may be because the resolution of the device is slightly affected because oxygen is a very light element compared to the other constituents of the compound.

Measurements of magnetic susceptibility as a

[DOI: 10.22068/ijmse.14.2.1]

Table 2. Compositional percentages of elements for Ba2GdSbO6 obtained from EDX.

Element	*Theoretical %*	*Experimental %*
Ba	42,28	43,33
Gd	24,20	24,81
Sb	18,74	19,10
O	14,78	12,76

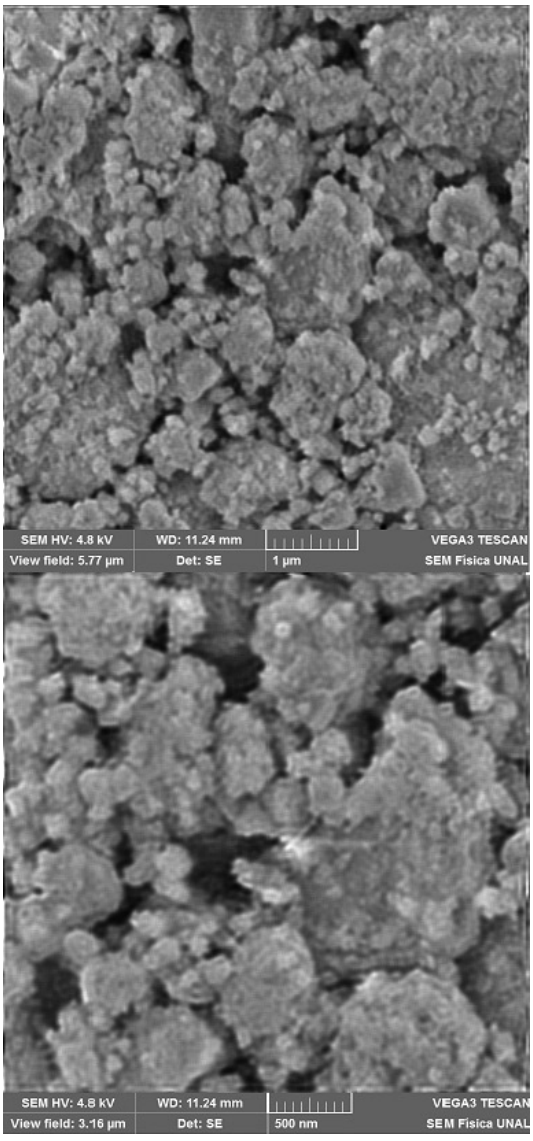

Fig. 3. Granular topology of the surface obtained from SEM images for the Ba_2GdSbO_6 perovskite-like material

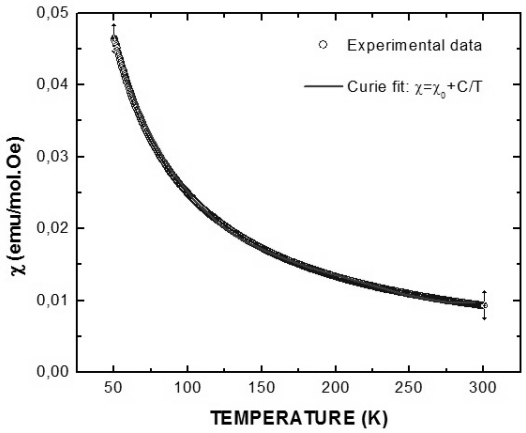

Fig. 4. Magnetic behaviour of Ba_2GdSbO_6 material obtained from measurements of susceptibility as a function of temperature. Red line corresponds to the fit with the Curie law.

function of temperature reveal the paramagnetic character of the Ba_2GdSbO_6 complex perovskite. Figure 4 shows the Curie fitting performed following the equation $X=X_0+(C/T)$. In the Curie equation, $C=N\mu^2_{eff}/3K_B$ is the Curie constant, N is Avogadros's number, μ_{eff} is the effective magnetic moment ($\mu_{eff}=P_{eff}\mu_B$), P_{eff} represent the effective Bohr magneton number, μ_B is the Bohr magneton, K_B is the Boltzmann constant and x_0=0,00139 emu/mol is the temperature independent susceptibility term. From the Curie constant C the effective magnetic moments for Ba_2GdSbO_6 material was calculated to be 8,1 μ_B. This value is 98% in agreement with the theoretical expected moments obtained from the Hund's rules [19]. The difference is attributed to other magnetic effects due to the hybridization of

[DOI: 10.22068/ijmse.14.2.1]

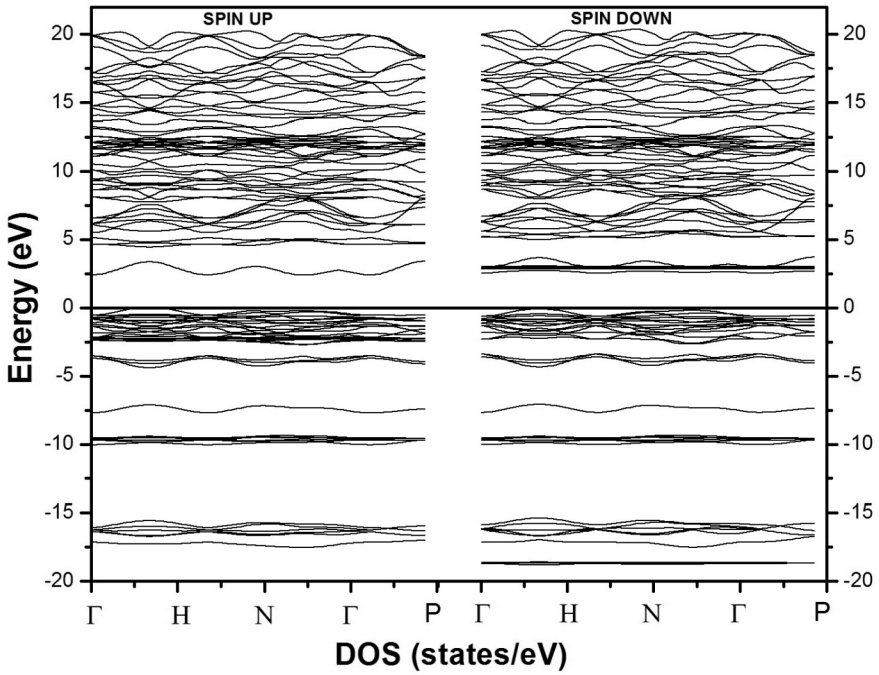

Fig. 5. Spin polarized band structure for the Ba_2GdSbO_6 double perovskite.

the d-Sb and f-Gd orbital and non-preferential spin orientations in the GdO_6 and SbO_6 octahedra due structural distortions.

In order to obtain the most accurate result, the optimal lattice parameter corresponding to the minimal energy value was calculated as the total energy versus volume. The total energy was calculated by fittings with the Murnaghan's state equation [15]. From total energy as a function of volume the ideal lattice parameter was determined to be a=6,0840 Å. Figure 5 shows the band structure for both up and down spin polarizations. In the picture, E=0 eV corresponds to the Fermi level. It is observed that these materials evidence weak semiconductor behavior with gap energy through the Fermi level from -0,05 eV up to 2,81 eV (width 2,86 eV) for the spin up polarization and between -0,05 eV and 2,78 eV (width 2,83 eV) for the spin down orientation.

The Partial Densities of States (DOS) for the Ba_2GdSbO_6 complex perovskite are exemplified in figure 6. As in the figure 5, the energy zero corresponds to the Fermi level reference. It is important to elucidate that close the Fermi level there are contributions due to the O-2p hybridizations but Gd-4f spin up orbitals are responsible for priority contributions. Very incipient contributions of Sb-3d states are observed. This behavior can be clearly seen in Figures 5 and 6 in the energy range between -2,87 and -0,05 eV. Localized states attributed to Sb-3d, Ba-6s and O-2p appear far the Fermi level, below – 3,00 eV. On the other hand, in the conduction band, it is observed in figures 5 and 6 that available states are majority due to the Gd-4f spin down orbitals with very small contributions of the Sb-3d and O-2p spin up and down levels.

The magnetic moment of mixed charge density was calculated to be 7,0 μ_B for Ba_2GdSbO_6. This value is relatively different from the value obtained experimentally. However, an important element to be taken into account has to do with the clutter of Gd and Sb cations in the structure of the double perovskite, which can not only distorted octahedra but also modify the magnetic response of the material.

Results of diffuse reflectance experiments are shown in figure 7. Reflectance values were acquired at 1 nm intervals over the 300–2500 nm,

[DOI: 10.22068/ijmse.14.2.1]

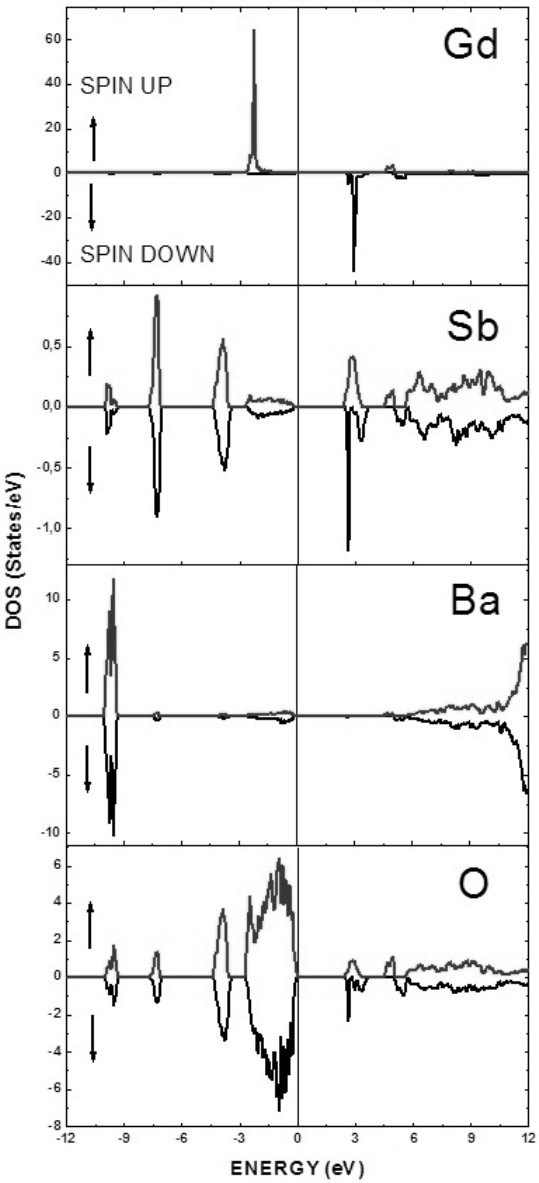

Fig. 6. Partial DOS with spin up and down polarizations for the Ba_2GdSbO_6 double perovskite.

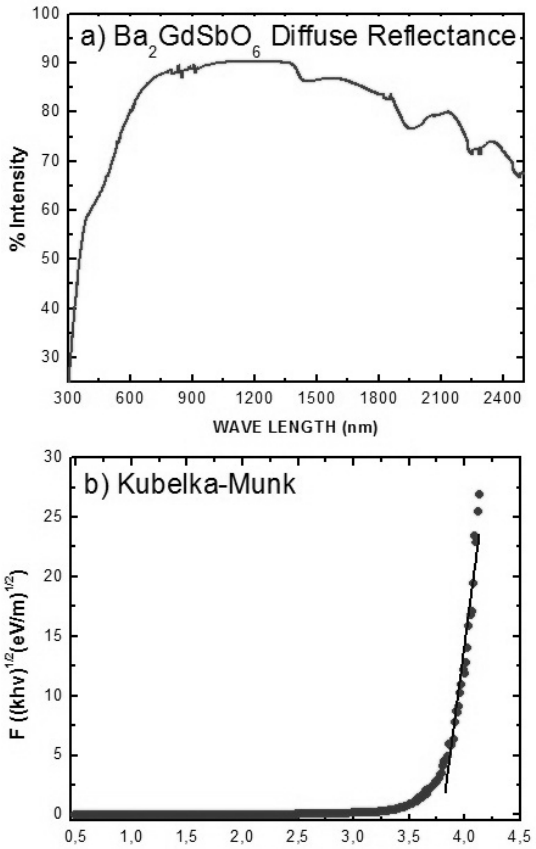

Fig. 7. a) Diffuse reflectance results for the Ba2GdSbO6 material. b) Kubelka–Munk fit.

as shown in figure 7a. The absorption of UV-Vis-NIR radiation reveals that the molecules of the Ba_2GdSbO_6 material cause the excitation of electrons from the ground state to exited state, which produces electronic jumps between quantum levels. The quantum characteristics energy, which depends from the electronic configuration, is calculated from the radiated energy. By applying the Kubelta-Munk model, currently used to the measurement of the band gap in powder samples, the respective band gap for the Ba_2GdSbO_6 perovskite is obtained as showed in figure 7b. Structural defects or vacancies can produce spontaneous absorption that appears for several wavelengths, as observed in figure 7a.

From the adjustment to the Kubelka–Munk equation it was determined that the energy gap of the Ba_2GdSbO_6 is 3,61 eV at room temperature, which is 33% different of the theoretic prediction given by the DOS calculations for T=0 K. This difference occurs because in the DFT calculations, the exchange and correlation potential by Perdew, Burke and Ernzerhof [14] gives a very good approximation for the valence and conduction density of states, but is not very accurate for determining the energy gap in

[DOI: 10.22068/ijmse.14.2.1]

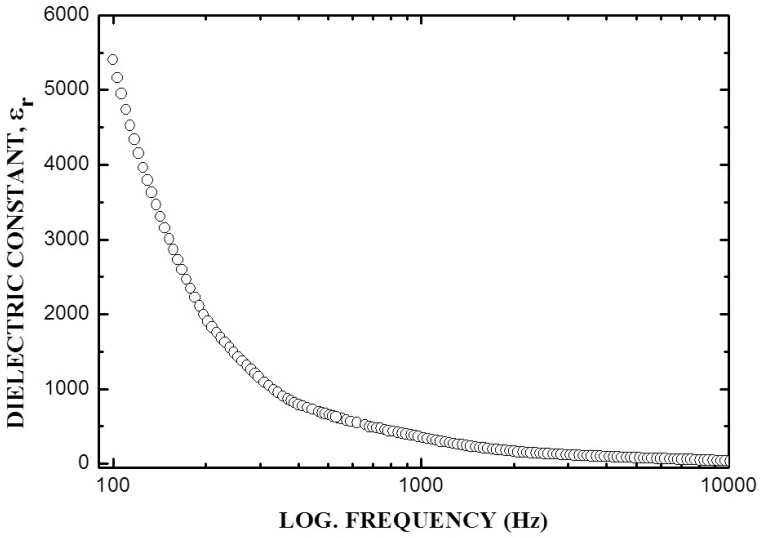

Fig. 8. Dielectric constant as a function frequency measured for the Ba_2GdSbO_6 perovskite.

semiconductors due to self-interaction errors [18-19], for which it would be more interesting to use a potential specifically designed for this purpose, that uses local functional without Hartree-Fock exchange [20-21].

The dielectric characteristics of this compound were obtained from measurements of the dielectric constant as a function of frequency performed. The corresponding results are shown in figure 8. As shown in the picture, at low frequencies (ν=100 Hz) the value of the dielectric constant ε_r=5400, which is a tendency of the giant-dielectric materials [22]. The value of the dielectric constant decreases dramatically with increasing frequency between 100 Hz and 1000 Hz. Above ν=1000 Hz, the dielectric constant decreases smoothly to the value ε_r=40 at ν=10 kHz. There are reports according to which it is expected that most giant dielectric constants are due interconnected effects of polarization [23]. In semiconductors, for example, the formation of Schottky barriers at the contacts could lead to depletion regimes. Another example has to do with the formation of internal barrier layer capacitors through grain boundaries, which produce relaxations Maxwell-Wagner type, resulting in very high dielectric constant [24]. It is not excluded that the behavior of the dielectric constant depending on the frequency has to do with the occurrence of relaxation processes attributed to hopping of oxygen O^{2-} ions and $(O2)^{2-}$ peroxide between multiple off-center sites of the crystal [22].

5. CONCLUSIONS

The Ba_2GdSbO_6 complex has been synthesized by the solid-state reaction procedure. A study of the crystalline and electronic structure was performed through the Linearized Augmented Plane Wave method (FP-LAPW) into the framework of the Density Functional Theory (DFT). The results reveal that a rhombohedral perovskite is the more stable structure with a lattice parameter a=6,0840 Å. Close to the Fermi level a mean energy gap of 2,84 eV was observed for both up and down spin polarizations, which permitted to classify this material as insulator. The largest contribution to the effective magnetic moment, due to the Gd^{3+} cations, evidenced a value of 7,0 μ_B. The crystalline structure was experimentally determined by means measurements in a Panalytical XPert Pro X-ray diffractometer with a Rietveld refinement of the diffraction pattern through de GSAS code. The experimental lattice parameter a=5,9882(1) Å is 98,4% in agreement with those theoretically predicted. Measurements

[DOI: 10.22068/ijmse.14.2.1]

of magnetic susceptibility as a function of temperature reveal the paramagnetic feature of this material. From the fitting with the Curie law the effective magnetic moment was obtained to be 8,1μ_B, which is slightly higher that the theoretical value for the Gd^{3+} isolated cation predicted by $\mu_{eff}=g[J(J+1)^{½}$, where g represents the Landé's factor and J is the quantic number related to the 4f electronic orbital. Experiments of diffuse reflectance and fittings with the Kubelka–Munk equation permitted to obtain an energy gap of 3,61 eV, which differs 33% when compared with the theoretical value predicted by DFT. This difference is attributed to the temperature effect.

ACKNOWLEDGEMENTS

This work was partially supported by DIB, Universidad Nacional de Colombia.

REFERENCES

1. Corredor, L. T., Roa-Rojas, J., Landínez Téllez, D. A., Beltrán, R., Pureur, P., Mesquita, F., Albino Aguiar, J., "Magnetic and structural properties of the new double perovskite family $Sr_2GdRu1-xRexOy$", J. Appl. Phys. 2013, 113, 17E302-17E305.
2. Llamosa, D. P., Landínez Téllez, D. A., Roa-Rojas, J., "Magnetic and structural behavior of Sr_2ZrMnO_6 double perovskite Physica B", 2009, 404, 2726-2729.
3. Macquart, R. B., Zhou, Q. D., Kennedy, B. J., Structural investigation of Sr_2LiReO_6. Evidence for a continuous tetragonal–cubic phase transition", Journal of Solid State Chem., 2009, 182, 1691-1693.
4. Glazer, A. M., "The classification of tilted octahedra in perovskites", Acta Crystallogr. Sect. B, 1972, 28, 3384-3392.
5. Glazer, A. M., "Simple ways of determining perovskite structures", Acta Crystallogr. Sect. A, 1975, 31, 756-762.
6. Woodward, P. M., "Octahedral Tilting in Perovskites I. Geometrical Considerations", Acta Crystallogr. Sect. B, 1997, 53, 32-43.
7. Howard, C. J., Kennedy, B. J., Woodward, P. M., "Structures of ordered double perovskites: A group theoretical analysis", Acta Crystallogr. B, 2003, 59, 463-471.
8. Wakeshima, M., Harada, D., Hinatsu, Y., Crystal structures and magnetic properties of ordered perovskites $A_2R_3+Ir_5+O_6$ (A=Sr, Ba; R=Sc, Y, La, Lu), J. Alloy and Compd., 1999, 287, 130-136.
9. Wakeshima, M., Harada, D., Hinatsu, Y., Masaki, N., "Magnetic Properties of Ordered Perovskites Ba_2LnIrO_6 (Ln=Sm, Eu, Gd, and Yb)", J. Solid State Chem. 1999, 147, 618-623.
10. Wakeshima, M., Harada, D., Hinatsu, Y., "Crystal structures and magnetic properties of ordered perovskites Ba_2LnIrO_6 (Ln = lanthanide)", J. Mater. Chem. 2000, 10, 419-422.
11. Cardona, R., Landínez Téllez, D. A., Arbey Rodríguez M., J., Fajardo, F., Roa-Rojas, J., "Structural and magnetic properties of double-perovskite Ba_2MnMoO_6 by density functional theory", J. Magn. Magn. Mater. 2008, 320, e85-e87.
12. Larson, A. C., von Dreele, R. B., "General Structure Analysis System (GSAS)", Los Alamos National Laboratory Report LAUR, 2000, pp. 86-748.
13. Blaha, P., Schwarz, K., Madsen, G. K. H., Kvasnicka, D., Luitz, J., "WIEN2k, an Augmented Plane Wave + Local Orbitals Program for Calculating Crystal Properties. Karlheinz Schwarz", Techn. Universität Wien, Vienna, 2001. ISBN 3-9501031-1-2.
14. Perdew, J. P., Burke, S., Ernzerhof, M., "Generalized Gradient Approximation Made Simple", Phys. Rev. Let. 1996, 77, 3865-3868.
15. Murnaghan, F. D., "The Compressibility of Media under Extreme Pressures", Proc. Natl. Acad. Sci., USA., 1944, 30, 244-247.
16. Lufaso, M. W., Woodward, P. M., "Prediction of the crystal structures of perovskites using the software program SPuDS", Structural Science, 2001, 57, 725-738.
17. Cullity, B. D., Graham, C. D., "Introduction to Magnetic Materials", 2nd Ed., IEEE Press, NJ, 2009.
18. Einollahzadeh, H., Dariani, R. S., Fazeli, S. M., "Computing the band structure and energy gap of penta-graphene by using DFT and G0W0 approximations", Solid State Commun. 2016,

[DOI: 10.22068/ijmse.14.2.1]

229, 1-4.

19. Zhao, Y., Truhlar, D. G., "Calculation of semiconductor band gaps with the M06-L density functional", J. of Chem. Phys. 2009, 130, 74103(1-3).
20. T. Higuchi, T. Tsukamoto, N. Sata, M. Ishigame, Y. Tezuka, S. Shin, "Electronic structure of p-type $SrTiO_3$ by photoemission spectroscopy", Phys. Rev. B, 1998, 57, 6978-6983.
21. N. Kulagin, J. Dojcilovic, D. Popovic, "Low-Temperature dielectric properties of doped $SrTiO_3$ single crystals and valency of ions", Cryogenics, 2001, 41, 745-750.
22. Lunkenheimer, P., Götzfried, T., Fichtl, R., Weber, S., Rudolf, T., Loidl, A., Reller, A., Ebbinghaus, S. G., "Apparent giant dielectric constants, dielectric relaxation, and ac-conductivity of hexagonal perovskites $La_{1.2}Sr_{2.7}BO_{7.33}$ (B=Ru, Ir)", J. of Solid State Chem. 2006, 179, 3965-3973.
23. Lunkenheimer, P., Fichtl, R., Ebbinghaus, S. G., Loidl, A., "Nonintrinsic origin of the colossal dielectric constants in $CaCu_3Ti_4O12$", Phys. Rev. B, 2004, 70, 172102.
24. Sinclair, D. C., Adams, T. B., Morrison, F. D., West, A. R., "$CaCu_3Ti_4O_{12}$ One-Step Internal Barrier Layer Capacitor", Appl. Phys. Lett., 2002, 80, 2153-2155.

[DOI: 10.22068/ijmse.14.2.1]